Applied Mathematics and Mechanics
(English Edition, Vol 26, No 2, Feb 2005)

Published by Shanghai University,
Shanghai, China

©Editorial Committee of Appl. Math. Mech., ISSN 0253-4827

Article ID: 0253-4827(2005)02-0242-10

PERTURBATIONAL FINITE VOLUME METHOD FOR THE SOLUTION OF 2-D NAVIER-STOKES EQUATIONS ON UNSTRUCTURED AND STRUCTURED COLOCATED MESHES*

GAO Zhi (高 智), DAI Min-guo (代民果)

LI Gui-bo (李桂波), BAI Wei (柏 威)

(Institute of Mechanics, Chinese Academy of Sciences,
Beijing 100080, P.R. China)

(Communicated by DAI Shi-qiang)

Abstract: *Based on the first-order upwind and second-order central type of finite volume (UFV and CFV) scheme, upwind and central type of perturbation finite volume (UPFV and CPFV) schemes of the Navier-Stokes equations were developed. In PFV method, the mass fluxes of across the cell faces of the control volume (CV) were expanded into power series of the grid spacing and the coefficients of the power series were determined by means of the conservation equation itself. The UPFV and CPFV scheme respectively uses the same nodes and expressions as those of the normal first-order upwind and second-order central scheme, which is apt to programming. The results of numerical experiments about the flow in a lid-driven cavity and the problem of transport of a scalar quantity in a known velocity field show that compared to the first-order UFV and second-order CFV schemes, upwind PFV scheme is higher accuracy and resolution, especially better robustness. The numerical computation to flow in a lid-driven cavity shows that the under-relaxation factor can be arbitrarily selected ranging from 0.3 to 0.8 and convergence perform excellent with Reynolds number variation from 10^2 to 10^4.*

Key words: colocated grid; structured grid; unstructured grid; perturbation finite volume method; incompressible fluid NS equations; SIMPLEC algorithm; MSIMPLEC algorithm; SIMPLER algorithm

Chinese Library Classification: O351 **Document code**: A

2000 Mathematics Subject Classification: 65N30

Introduction

The finite volume (FV) method uses the integral form of the conservation equation as its starting point and can utilize conveniently diversified grids (structured and unstructured grids) and

* **Received date**: 2003-01-21; **Revised date**: 2004-10-22
Foundation item: the National Natural Science Foundation of China (10032050, 10272106)
Biographies: GAO Zhi, Professor; DAI Min-guo, E-mail: 20108009@sina.com

万方数据

is suitable for very complex geometry, which are why it is popular with engineering and has been widely used in a great variety of commercial software of computational fluid dynamics. Relative to the finite element (FE) method and the finite differential (FD) method, the disadvantage of FV method is that it is not higher accuracy. FV method is of second level approximation, namely, integral approximation and reconstruction approximation. If the integral approximation is of n_1-order accuracy and reconstruction approximation is of n_2-order accuracy, the order accuracy of FV method is the smaller one in n_1 and n_2. Civil and foreign researchers have made a lot of efforts to develop all kinds of practical FV schemes, for example, first-order upwind and second-order center differential schemes[1], center type FV scheme by Jameson[2,3] and AUSM by Liou and Steffen[4,5]. But its accuracy is lower than or equal to second-order accuracy. In general, FV schemes whose accuracy is higher than second-order are multi-node scheme. Because of multi-node scheme referring to more control volumes and corresponding to solve more complicated algebra equations, it is very difficult to be used in the three-dimensional cases.

In recent years, Z. Gao[6,7] presented perturbation finite volume (PFV) method which is different from conventional ones that improve scheme accuracy. Coventional methods separately process convectional term and diffuse term in governing equations while PFV method considers them as a whole and improves numerical scheme accuracy by means of inherent association in them. In detail, the numerical mass fluxes of across the cell faces were expanded into power series of the grid spacing and the coefficients of the power series were determined with the aid of the integral conservation equation itself. Finally, upwind and central type of PFV schemes for convection and diffuse equations were obtained. It retains the advantages of the first-order upwind and second-order central FV scheme, however, its interpolation (or call it reconstruction) approximation are of arbitrary order accuracy. Numerical tests of the problem of transport of a scalar quantity in a known velocity field and several model equations with PFV scheme used show that PFV schemes have higher accuracy and higher resolution, better stability and wider applicable range of Reynolds number than those of the normal first-order upwind scheme.

In this paper, the PFV method for the Navier-Stokes equations for incompressible fluid flow is developed. The cavity flow in a lid driven is computed with the hybrid algorithm including SIMPLER[8] and MSIMPLEC[9] used in structured grid and with the SIMPLEC[10] algorithm used in unstructured grid, which are used to predict the pressure-velocity coupling correction, sixth-order upwind PFV and first-order upwind FV used. The problem of transport of a scalar auantity in a known velocity field was solved numerically with second-order upwind PFV, forth-order central PFV, second-order central FV and first-order upwind FV schemes respectively used. Comparison in numerical results of the above-cited several schemes is given and discussed.

1 Perturbational Finite Volume (PFV) Scheme

The general form of a scalar transport integral equation is

$$\frac{\partial}{\partial t}\int_V \rho\phi \mathrm{d}V + \int_S \rho\phi \boldsymbol{u}\cdot\boldsymbol{n}\mathrm{d}S = \int_S \mu\nabla\phi\cdot\boldsymbol{n}\mathrm{d}S, \tag{1}$$

where ϕ is the general scalar variable; ρ, $\boldsymbol{u}$, t and μ are the fluid density, velocity, time and dynamic viscosity, respectivemy; V and S are respectively the volume and surface area of control volume (CV); $\boldsymbol{n}$ is the normal unit vector of the cell face. The perturbational finite volume

万方数据

(PFV) method uses the first-order upwind and second-order central FV scheme for the convective-diffusion integral equation as its starting point. The mass fluxes across each face of the control volume are modified and expanded into power-series of the grid spacing. The coefficients of the power-series are determined with the use of a space splitting technique and the relations between the convective and diffusion fluxes. In the case of that the line connecting two central nodes P_0 and P_j of adjacent control volumes is nearly orthogonal to the common face owned by control volume P_0 and control volume P_j, the semi-discretized upwind and central type of PFV scheme is deduced as

$$\frac{\partial}{\partial t}(V_{P_0}\phi_{P_0}) = \sum_{j=1}^{n_{P_0}} \frac{1}{G_j}\left[\mu\frac{\boldsymbol{d}_j\cdot\boldsymbol{S}_j}{|\boldsymbol{d}_j|^2} - \frac{1}{2}\dot{m}_{jf}(1-\mathrm{sign}\dot{m}_{jf})\sum_{k=0}^{N}\frac{(-1)^k}{(k+1)!}R_{jf}^k\right](\phi_{P_j}-\phi_{P_0}) -$$

$$\sum_{j=1}^{n_{P_0}} p_j S_j + \sum_{j=1}^{n_{P_0}} \frac{1}{G_j}\left[(\mu\nabla\phi\cdot\boldsymbol{S})_j - \mu\frac{\boldsymbol{d}_j\cdot\boldsymbol{S}_j}{|\boldsymbol{d}_j|^2}(\phi_{P_j}-\phi_{P_0})\right]^{\mathrm{old}} = 0, \tag{2}$$

$$G_j = \sum_{k=0}^{N}\frac{1}{(k+1)!}R_{jf}^k(\mathrm{sign}\dot{m}_{jf})^k, \tag{3}$$

$$\mathrm{sign}\dot{m}_{jf} = \begin{cases} 1, & \dot{m}_{jf} > 0, \\ -1, & \dot{m}_{jf} < 0, \end{cases} \tag{4}$$

$$\frac{\partial}{\partial t}(V_{P_0}\phi_{P_0}) = \sum_{j=1}^{n_{P_0}} \frac{1}{G_j^c}\left[\mu\frac{\boldsymbol{d}_j\cdot\boldsymbol{S}_j}{|\boldsymbol{d}_j|^2} - \frac{1}{2}\dot{m}_{jf}\sum_{k=0}^{2N+1}\frac{(-1)^k}{(k+1)!}R_{jf}^k\right](\phi_{P_j}-\phi_{P_0}) -$$

$$\sum_{j=1}^{n_{P_0}} p_j S_j + \sum_{j=1}^{n_{P_0}} \frac{1}{G_j^c}\left[(\mu\nabla\phi\cdot\boldsymbol{S})_j - \mu\frac{\boldsymbol{d}_j\cdot\boldsymbol{S}_j}{|\boldsymbol{d}_j|^2}(\phi_{P_j}-\phi_{P_0})\right]^{\mathrm{old}} = 0, \tag{5}$$

$$G_j^c = \sum_{k=0}^{N}\frac{1}{(2k+1)!}R_{jf}^{2k}, \tag{6}$$

where ϕ_{P_0} is the value of ϕ at the central node of the control volume P_0, V_{P_0} is the volume of the control volume P_0, $\boldsymbol{d}_j$ is the vector linking two adjacent control volume center with directional being from P_0 to P_j, $\boldsymbol{S}_j$ is the area-vector of the jf-face on the boundary of control volume P_0 and its directional agrees with the outer normal of that face, $R_{jf} = F_{jf}\cdot|\boldsymbol{d}_j|^2/(\mu\boldsymbol{d}_j\cdot\boldsymbol{S}_j)$ can be considered as the cell Reynolds number in the $\boldsymbol{d}_j$-direction, $\dot{m}_{jf}$ is the mass flux of across the cell jf-face. The continuity equation of fluid flow of across the cell gives as follows:

$$\sum_{j=1}^{n_{P_0}}\dot{m}_{jf} = 0. \tag{7}$$

The last term in the right-hand side of the PFV schemes (2) and (5), labeled old, is computed in the previous iteration and it is usually very small because the line connecting two adjacent control volume center P_0 and P_j is nearly orthogonal to the common face. From the treatment of deducing the PFV scheme, we know that the truncation-error of the modified differential equation of the upwind PFV and central PFV scheme respectively is of $(N+1)$th-order and $(2N+2)$th-order. Therefore, the upwind PFV scheme (2) is a mixed one with $(N+1)$th-order interpolation and second-order integration approximations while the central PFV scheme (5) is a mixed one with $(2N+2)$th-order interpolation and second-order integration approximations. If let $N = 0$ in the relations (2) and (5), the upwind PFV and the second

万方数据

central PFV schemes respectively is reduced to the normal first-order upwind FV and second-order central FV scheme for the integral equation (1). Remarkably, the UPFV scheme (2) inherits the TVD character owned inherently by first-order upwind FV scheme and the second-order central PFV scheme (5) is cell-centered positive one for any value of the grid Peclet number. In addition, $|\boldsymbol{d}_j|$ is the length of the vector pointing from the center of control volume P_0 to the centre of adjacent control volume P_j. The *jf*-face on the boundary of control volume P_0 is the common face of the two adjacent control volumes P_0 and P_j. If $\delta_j |\boldsymbol{d}_j|$ notes the distance from the center node P_0 to the *jf*-face and $(1-\delta_j)|\boldsymbol{d}_j|$ notes the distance from the node P_j to the *jf*-face, the PFV scheme with distance factor $\delta_j \neq 1/2$ is the same as that with distance factor $\delta_j = 1/2$. In general, the δ_j is often not equal to $(1-\delta_j)$ for the great majority of unstructured and unstructured-structured mixed grids. This is a good property of the PFV schemes (2) and (5), which cause terse expression and easy programming.

2 Perturbational Finite Volume (PFV) Scheme of N-S Equations

The integral form of the Navier-Stokes (NS) equations for the two-dimensional, steady, incompressible flow are

$$\int_S \rho \boldsymbol{u}\cdot\boldsymbol{n}\mathrm{d}S = 0, \tag{8}$$

$$\int_S \rho\phi\boldsymbol{u}\cdot\boldsymbol{n}\mathrm{d}S = -\int_S p\boldsymbol{n}\mathrm{d}S + \int_S \mu\nabla\phi\cdot\boldsymbol{n}\mathrm{d}S, \tag{9}$$

where $\boldsymbol{u} = (u, v)$, u and v are respectively the velocity components in the Cartesian x- and y-coordinate directions, p denotes the pressure.

2.1 PFV scheme of the NS momentum equation (9)

In the case of that the line connecting two center nodes of the two adjacent control volumes P_0 and P_j is nearly orthogonal to the common *jf*-face, the upwind and central PFV scheme for the NS momentum equation (9) is respectively deduced is

$$\sum_{j=1}^{n_{P_0}} \frac{1}{G_j}\left[\mu\frac{\boldsymbol{d}_j\cdot\boldsymbol{S}_j}{|\boldsymbol{d}_j|^2} - \frac{1}{2}\dot{m}_{jf}(1-\mathrm{sign}\dot{m}_{jf})\sum_{k=0}^{N}\frac{(-1)^k}{(k+1)!}R_{jf}^k\right](\phi_{P_j}-\phi_{P_0}) - \sum_{j=1}^{n_{P_0}} p_j S_j + \sum_{j=1}^{n_{P_0}}\frac{1}{G_j}\left[(\mu\nabla\phi\cdot\boldsymbol{S})_j - \mu\frac{\boldsymbol{d}_j\cdot\boldsymbol{S}_j}{|\boldsymbol{d}_j|^2}(\phi_{P_j}-\phi_{P_0})\right]^{\mathrm{old}} = 0, \tag{10}$$

$$\sum_{j=1}^{n_{P_0}} \frac{1}{G_j^c}\left[\mu\frac{\boldsymbol{d}_j\cdot\boldsymbol{S}_j}{|\boldsymbol{d}_j|^2} - \frac{1}{2}\dot{m}_{jf}\sum_{k=0}^{2N+1}\frac{(-1)^k}{(k+1)!}R_{jf}^k\right](\phi_{P_j}-\phi_{P_0}) - \sum_{j=1}^{n_{P_0}} p_j S_j + \sum_{j=1}^{n_{P_0}}\frac{1}{G_j^c}\left[(\mu\nabla\phi\cdot\boldsymbol{S})_j - \mu\frac{\boldsymbol{d}_j\cdot\boldsymbol{S}_j}{|\boldsymbol{d}_j|^2}(\phi_{P_j}-\phi_{P_0})\right]^{\mathrm{old}} = 0, \tag{11}$$

in which the term, labeled old, is computed in the previous iteration. The expressions of G_j and G_j^c are respectively from the formulae (3) and (6). Above equation is finally expressed as

$$a_0\phi_{P_0} = \sum_{j=1}^{n_{P_0}} a_j\phi_{P_j} + b_0, \tag{12}$$

where

万方数据

$$a_j = \frac{1}{G_j}\left[\mu\frac{\boldsymbol{d}_j\cdot\boldsymbol{S}_j}{|\boldsymbol{d}_j|^2} - \frac{1}{2}\dot{m}_{jf}(1-\mathrm{sign}\dot{m}_{jf})\sum_{k=0}^{N}\frac{(-1)^k}{(k+1)!}R_{jf}^k\right] \quad \text{or}$$

$$\frac{1}{G_j^c}\left[\mu\frac{\boldsymbol{d}_j\cdot\boldsymbol{S}_j}{|\boldsymbol{d}_j|^2} - \frac{1}{2}\dot{m}_{jf}\sum_{k=0}^{2N+1}\frac{(-1)^k}{(k+1)!}R_{jf}^k\right], \tag{13}$$

$$a_0 = \sum_{j=1}^{n_{P_0}} a_j, \tag{14}$$

$$b_0 = -\sum_{j=1}^{n_{P_0}} p_j\boldsymbol{S}_j + \sum_{j=1}^{n_{P_0}}\frac{1}{G_j}\left[(\mu\nabla\phi\cdot\boldsymbol{S})_j - \mu\frac{\boldsymbol{d}_j\cdot\boldsymbol{S}_j}{|\boldsymbol{d}_j|^2}(\phi_{P_j}-\phi_{P_0})\right]^{\mathrm{old}} \quad \text{or}$$

$$-\sum_{j=1}^{n_{P_0}} p_j\boldsymbol{S}_j + \sum_{j=1}^{n_{P_0}}\frac{1}{G_j^c}\left[(\mu\nabla\phi\cdot\boldsymbol{S})_j - \mu\frac{\boldsymbol{d}_j\cdot\boldsymbol{S}_j}{|\boldsymbol{d}_j|^2}(\phi_{P_j}-\phi_{P_0})\right]^{\mathrm{old}}. \tag{15}$$

The under-relaxation is always used in the numerical computation to avoid the divergence of the iterative procedure[11]. Therefore the following equation is to be solved:

$$\left(\frac{a_0}{\alpha_\phi}\right)\phi_{P_0} = \sum_{j=1}^{n_{P_0}} a_j\phi_{P_j} + b_0 + (1-\alpha_\phi)\frac{a_0}{\alpha_\phi}\phi_{P_0}^{\mathrm{old}}, \tag{16}$$

where α_ϕ is the under-relaxation factor for the variable ϕ. It is equal to 0.6 for two velocity components u and v. The under-relaxation factor for pressure is also set to 0.6.

2.2 The pressure-velocity coupling correction equation and its numerical discretization

Regarded the pressure $p_{P_0}^*$ determined in the previous iteration as the initial value of the present iteration, the initial velocity $\boldsymbol{u}_{P_0}^*$ can be obtained by solving the discretized momentum equation (16), which is not necessary to satisfy the continuity equation (7). To avoid uncoupling between pressure and velocity, the initial velocity and pressure value must be corrected. Here, the hybrid algorithm including SIMPLER and MSIMPLEC thought is adopted for structured grid while SIMPLEC algorithm is used for unstructured grid. The following discussion is emphasized on hybrid algorithm including MSIMPLEC and SIMPLER thoughts. Based on the MSIMPLEC algorithm, the cell face modified velocity $\boldsymbol{u}_j'$ is defined as

$$\boldsymbol{u}_j' = -\frac{1}{2}\left[\left(\frac{V}{a_0'}\right)_{P_0} + \left(\frac{V}{a_0'}\right)_{P_j}\right]\left(\frac{p_{P_j}' - p_{P_0}'}{|\boldsymbol{d}_j|}\right)\frac{\boldsymbol{S}_j}{|\boldsymbol{S}_j|}, \tag{17}$$

$$a_0' = \frac{a_0}{\alpha_\phi} - \sum_{j=1}^{n_{P_0}} a_j, \tag{18}$$

where p_{P_0}' and p_{P_j}' are the pressure corrections of the control volume (CV) P_0 and P_j, respectively. The linear interpolation of the initial velocity $\boldsymbol{u}_{P_0}^*$ is adopted to obtain the cell face velocity $\boldsymbol{u}_j^*$. Then $\boldsymbol{u}_j'$ should make $(\boldsymbol{u}_j^* + \boldsymbol{u}_j')$ satisfy the continuity equation. Substituting above equation into the continuity equation, we can reach the following discretized equation about the pressure correction p_{P_0}':

万方数据

$$a_0^p p'_{P_0} = \sum_{j=1}^{n_{P_0}} a_j^p p'_{P_j} + b_0^p, \tag{19}$$

where the superscript p denotes that the coefficients are in the pressure-correction equation. And the coefficients are given by

$$a_j^p = \frac{1}{2}\left[\left(\frac{V}{a_0'}\right)_{P_0} + \left(\frac{V}{a_0'}\right)_{P_j}\right]\frac{|S_j|}{|d_j|}, \tag{20}$$

$$a_0^p = \sum_{j=1}^{n_{P_0}} a_j^p, \tag{21}$$

$$b_0^p = -\sum_{j=1}^{n_{P_0}} F_j, \tag{22}$$

where b_0^p denotes the sum of mass fluxes through the faces of the CV P_0. After obtained the pressure correction p'_{P_0}, the pressure and the velocity are corrected by

$$p_{P_0} = p^*_{P_0} + \alpha_p p'_{P_0}, \tag{23}$$

$$\boldsymbol{u}_{P_0} = \boldsymbol{u}^*_{P_0} - \frac{V_{P_0}}{a_0^u}\nabla p'_{P_0} = \boldsymbol{u}^*_{P_0} - \sum_{j=1}^{n_{P_0}} \frac{p'_j \boldsymbol{S}_j}{a_0^u}, \tag{24}$$

where α_p is the under-relaxation factor for the pressure, which is given 0.6 here. Following that, according to MSIMPLEC algorithm, velocity field will be explicitly corrected by means of momentum equation.

$$\boldsymbol{u}_{P_0} = \left(\sum_{j=1}^{n_{P_0}} a_p^j \boldsymbol{u}_p^j - V_{P_0}\nabla p\right)^{\text{old}} / a_0^u. \tag{25}$$

After that, according to SIMPLER thought, pressure will be solved directly. This is corresponding to modify the predict pressure by MSIMPLEC. The equation computed directly pressure in SIMPLER is the same appearance as one computed modified pressure in MSIMPLEC. But coefficient and quality residual must be computed by $\boldsymbol{u}_{P_0}$ just corrected explicitly.

3 Numerical Tests

3.1 Flow in a lid-driven cavity

The viscous flow in a lid-driven cavity was computed for the case of Re = 1 000, 3 200, 5 000 with the cell-centered sixth-order upwind PFV, second-order central FV and first-order upwind FV schemes, the hybrid algorithm including MSIMPLEC and SIMPLER thought and uniform structured grid used. For the case of Re = 1 000, the flow was again computed with SIMPLEC algorithm, unstructured grid, sixth-order UPFV and first-order UFV used. Above the two cases, the algebraic equation system is solved by the Gauss-Seidel method. The inner iterations are set to four. The result is compared with those of the Ghia solution[12].

Figures 3 ~ 10 gives the horizontal and vertical velocity components u and v at the vertical and horizontal centerlines of the cavity with Reynolds number set 1 000, 3 200 and 5 000, respectively. In the case of Reynolds number being 1 000, the result of upwind PFV is nearly coinciding with that of Ghia both structured grid and unstructured grid respectively used. The

万方数据

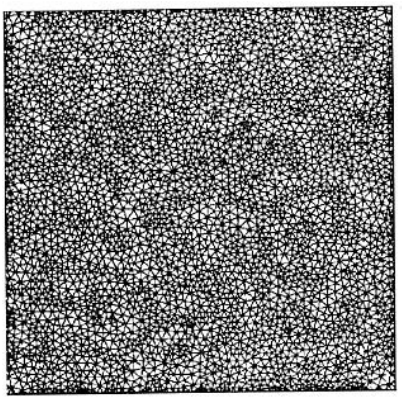

Fig.1 Unstructured mesh for the flow in a lid-driven cavity

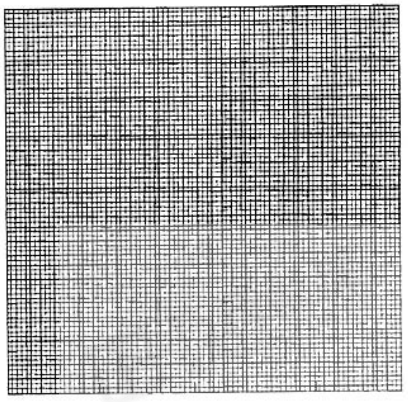

Fig.2 Uniform grid for the flow in a lid-driven cavity

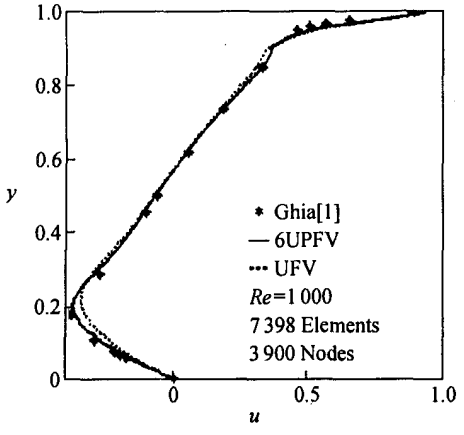

Fig.3 Horizontal velocity component u at the vertical centerline(unstructured mesh)

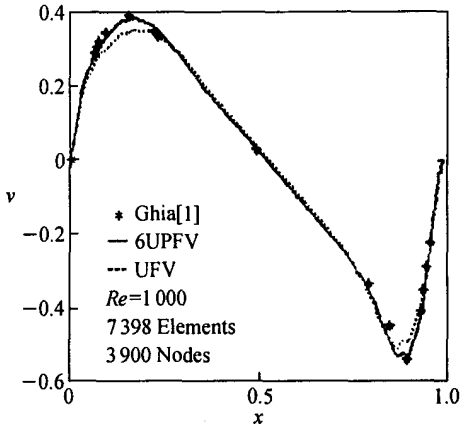

Fig.4 Vertical velocity component v at the horizontal centerline (unstructured mesh)

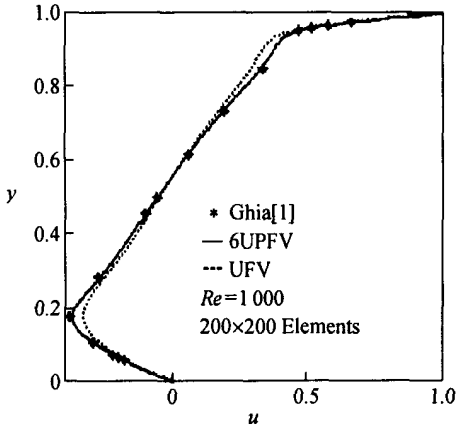

Fig.5 Horizontal velocity component u at the vertical centerline (structured grid)

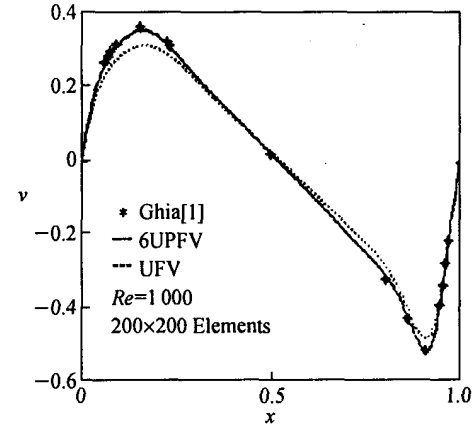

Fig.6 Vertical velocity component v at the horizontal centerline (structured grid)

万方数据

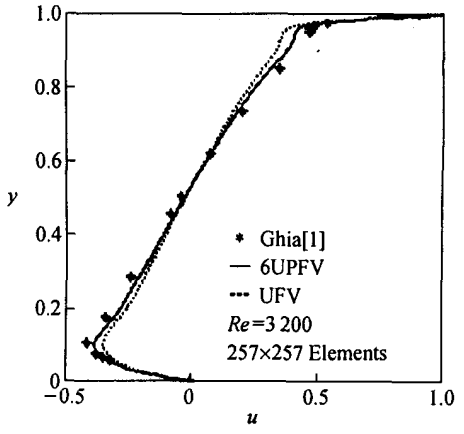

Fig.7 Horizontal velocity component u at the vertical centerline (structured grid)

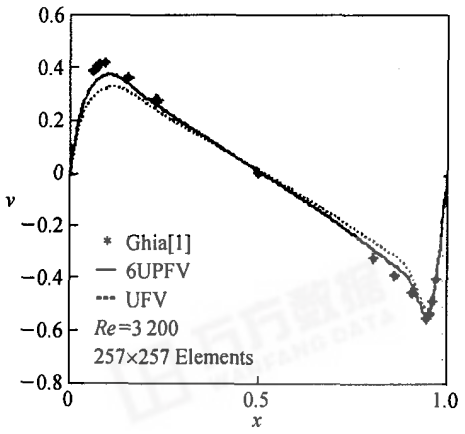

Fig.8 Vertical velocity component v at the horizontal centerline (structured grid)

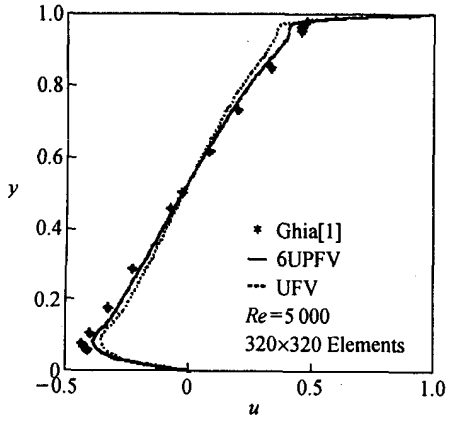

Fig.9 Horizontal velocity component u at the vertical centerline (structured grid)

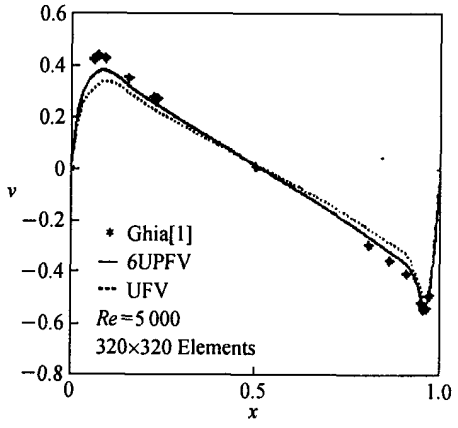

Fig.10 Vertical velocity component v at the horizontal centerline (structured grid)

computational results of PFV schemes match the Ghia solution well for Reynolds number set 3 200 and 5 000. But in the Ghia solution, the multi-structured grid technique was used. From Fig.3 to Fig.10, the accuracy of computation result of sixth-order upwind PFV is outstanding improvement comparison with that of UFV. In general, convergence become more difficult with grid refined. To avoid to lost generality, the global absolute mass fluxes residue and relative mass fluxes residue[13] convergence curves by different scheme were given out and compared with grids equal to 320 × 320 and Reynolds number equal to 5 000. From Fig.11, the relative mass fluxes residue curve by second central FV scheme is a great amplitude of oscillations when iterations are less than 1 000 while upwind PFV performs steadily. From Fig.12, although there are oscillations in convergences curves, amplitude correspond to UPFV is less and attenuate much faster. It is obvious that when convergence was reached, upwind PFV scheme saved about 1 500 outer iterations relative to upwind FV scheme.

万方数据

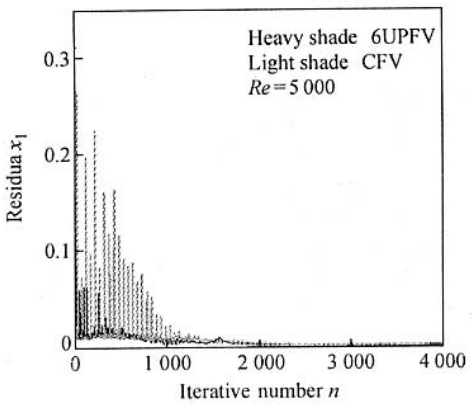

Fig.11 Global relative mass flux residue

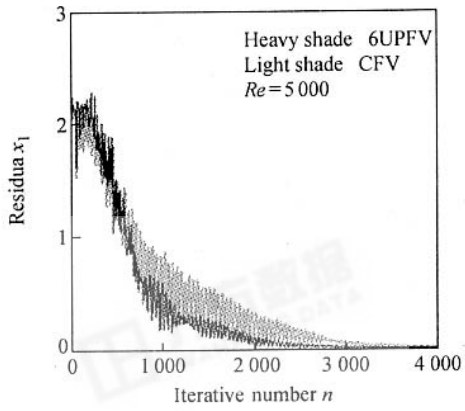

Fig.12 Global absolute mass flux residue

3.2 The problem of transport of a scalar quantity in a known velocity field

The governing equation is Eq.(1). The velocity field near a stagnation point ($x = 0$, $y = 0$) is given by $u = x$, $v = -y$. The following boundary conditions are to be imposed on: inlet ($y = 1$), $\phi = 0$; along the west boundary ($x = 0$), $\phi = 1 - y$; symmetry condition on the south boundary ($y = 0$), $\partial\phi/\partial y = 0$; outlet ($x = 1$), $\partial\phi/\partial x = 0$.

The isoclines of ϕ calculated on 40×40 CV using second-order UPFV for the convective fluxes with values of $\rho = 1.0$ and $\Gamma = 0.001$ is presented in Fig.13. In computation, for $\Gamma = 0.001$, if coarse grid is used, for example 10×10 CV, the second-order CFV will produce large oscillations and can not produce a convergence solution, while the second-order upwind PFV and forth-order central PFV scheme result in a meaningful solution with no oscillation. Although the first-order upwind FV produce a smooth convergence solution on a coarse grid, it is a higher error. The conclusions are visualized in Fig.14.

The diffusion fluxes across west wall varying with grid refined are given in Fig.14. It is apparent that second-order CFV scheme can not produce the meaningful convergence solution

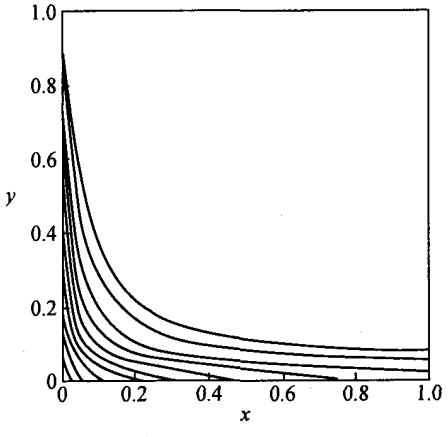

Fig.13 Isoclines of ϕ

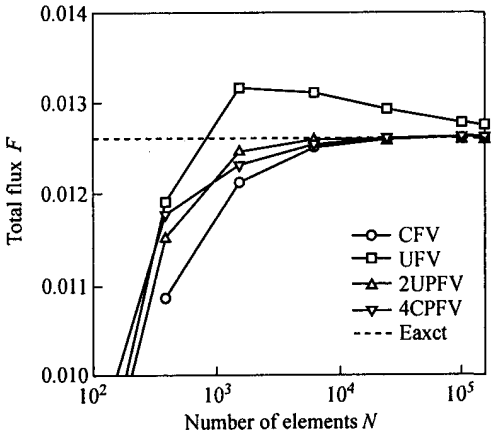

Fig.14 Convergence of total flux of ϕ through the west wall

万方数据

under the condition of coarse grid while second UPFV and forth CPFV can do. In the case of the same grid numbers, the solutions by PFV scheme are higher accuracy and faster convergence velocities than those by the UFV and CFV scheme.

4 Conclusions

Perturbation finite volume (PFV) scheme of the Navier-Stokes equations for incompressible flow is a terse and efficient formulations. It uses the same nodes as those of the normal first-order upwind and second-order central FV schemes. However, the reconstruction approximations of PFV scheme are of higher order accuracy. Numerical results of using upwind PFV schemes, first-order upwind and second-order central FV scheme to compute the flow in a lid-driven cavity show that the resolution and efficient of PFV scheme is higher than that of first-order upwind and second-order central FV scheme and the applicable range of Reynolds number of PFV scheme is much wider than that of second-order central FV scheme. Especially, it is better robustness. In numerical test with Reynolds number equal to 1 000, 3 200 and 5 000, respectively, underrelaxation factor is set to 0.6 and keep constant. In fact, the optional range for underrelaxation factor is wide and when the factor is arbitrarily selected from 0.3 to 0.8, convergence solution will also be obtained.

References:

[1] Ferziger J H, Peric M. *Computational Methods for Fluid Dynamics*[M]. 2nd ed. Springer, Berlin, 1999.

[2] Jameson A, Baker T J. Muligrid solution of the Euler equations for aircraft configurations[R]. AIAA-84-0093, 1984, 12.

[3] Jameson A, Yoon S. Lower-upper implicit schemes with multiplegrid for the Euler equations[J]. *AIAA J*, 1987, **25**(7): 929 – 935.

[4] Liou M, Steffen C J. A new flux splitting scheme[J]. *J Comput Phys*, 1993, **107**(1): 23 – 39.

[5] Liou M. A sequel to AUSM: AUSM$^+$ [J]. *J Comput Phys*, 1996, **129**(2): 364 – 382.

[6] Gao Zhi. Perturbational finite volume method for convective-diffusion equation and discussion[A]. In: Chinese Aerodynamics Research Society. *Proc 11th National Conference on Computational Fluid Dynamics*[C]. Luoyang, China, 2002, 29 – 35. (in Chinese)

[7] Gao Zhi, Xiang Hua, Shen Yiqing. Perturbational finite volume method and the significance of higher order accuracy of reconstruction approximation[J]. *Chinese Journal of Computational Physics*, 2004, **21**(2): 137 – 142. (in Chinese)

[8] Patankar S V. A calculation procedure for two-dimensional elliptic situations[J]. *Numer Heat Transfer*, 1981, **4**(4): 409 – 425.

[9] Yen R H, Liu C H. Enhancement of the SIMPLE algorithm by and additional explicit correction step [J]. *Numer Heat Transfer, Part B*, 1993, **24**(1): 127 – 141.

[10] Van Doormaal J P, Raithby G D. Enhancement of the SIMPLE method for predicting incompressible fluid flows[J]. *Numer Heat Transfer*, 1984, **7**(2): 147 – 163.

[11] Peric M. Analysis of pressure velocity coupling on nonorthogonal grids[J]. *Numer Heat Transfer, Part B*, 1990, **17**(1): 63 – 82.

[12] Ghia U, Ghia K N, Shin C T. High Re-solutions for incompressible flow using the Navier-Stokes equations and a multigrid method[J]. *J Comput Phys*, 1982, **48**(3): 387 – 411.

[13] Tao Weiquan. *The Numer Heat Transfer*[M]. 2th ed. Xi'an Jiaotong University Press, Xi'an, 2002, 5. (in Chinese)

万方数据